Medicinal Chemistry Research (2023) 32:2419–2431
https://doi.org/10.1007/s00044-023-03132-9

MEDICINAL CHEMISTRY RESEARCH

ORIGINAL RESEARCH ARTICLE

Synthesis, *in-silico* based virtual screening,anti-cancer potential of novel1,2,3-triazole-thiadiazole hybrid derivatives as Aurora kinase A (ARK-A) and Extracellular regulated kinase 2 (ERK2) dual inhibitors

Lingaiah Bontha[1] · Praveen Kumar Edigi[1] · Appaji Dokala[2,3] · Divya Pingili[4] · Venkat Reddy Putta[1] · Ravi kumar Vuradi[1] · Laxma Reddy Kotha[1] · Satyanarayana Sirasani[1]

Received: 14 March 2023 / Accepted: 25 July 2023 / Published online: 12 September 2023

Abstract

As part of our ongoing efforts to produce promising cytotoxic agents, the novel compounds, 5-(4-(diethylamino)-2-((1-substitutedphenyl-1*H*-1,2,3-triazol-4-yl)methoxy)phenyl)-1,3,4-thiadiazol-2-yl)pyrrolidine-2,5-dione derivatives (**9a-l**) were developed, synthesized, and characterized using several analytical techniques, including ^{1}H NMR, ^{13}C NMR, and LC-MS. New series of 1,2,3-triazole and thiadiazole molecular hybrids synthesized were evaluated for their anti-cancer activity against human esophageal carcinoma cell line KYSE-450 and human pancreatic carcinoma cell line MIA PaCa-2 cells. According to cytotoxic evaluation data, compounds **9b**, **9i**, **9j**, and **9l** exhibited potential cytotoxic activity against KYSE-450 and MIAPaCa-2 cells. Compound **9j** had more significant anti-cancer potential than the standard employed across all compounds evaluated. The remaining compounds exhibited moderate to weak anti-proliferative potential. In-vitro kinase inhibition of compound **9j** was significantly more effective against ARK-A and ERK2 enzymes, indicating its dual inhibition potential. Docking analysis showed that **9k, 9j**, and **9i** have substantial docking scores with the ARK-A receptor, indicating the presence of strong binding affinities. Significant binding interactions between molecules **9j** and **9h** and the ERK2 receptor suggest an inhibitory effect. Hence the compounds are promising dual inhibitors of ARK-A/ERK2.

Graphical Abstract

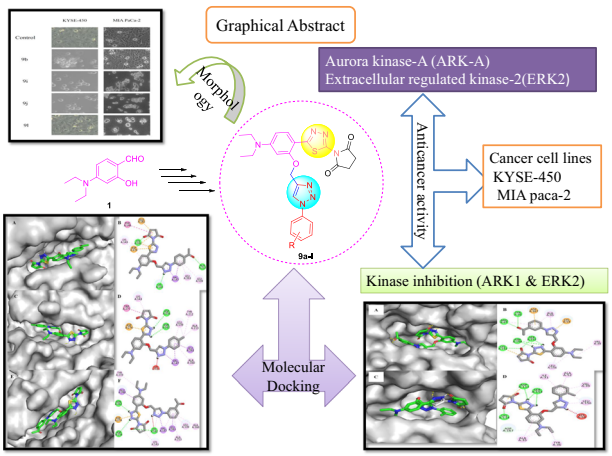

✉ Laxma Reddy Kotha
klreddy200542@gmail.com

✉ Satyanarayana Sirasani
ssnsirasani@gmail.com

[1] Department of Chemistry, University College of Science, Osmania University, Hyderabad, Telangana 500 007, India

[2] Center for Innovation in Molecular and Pharmaceutical Sciences (CIMPS), Dr Reedys Institute of Life Sciences, University of Hyderabad Campus, Gachibowli, Hyderabad, Telangana 500046, India

[3] Department of Molecular Therapeutics, PGP Life Sciences, IKP Knowledge Park, Turkapally, Telangana 500078, India

[4] Department of Pharmaceutical Chemistry, Sri VenkateshwaraColege of Pharmacy, Madhapur, Hyderabad, India

Keywords 1 · 2 · 3-triazole · Thiadiazole · Anticancer activity · ARK-A/ERK2 · Dual inhibitors

Introduction

Cancer is widely recognized as a highly perilous and potentially fatal ailment on a global scale. It ranks as the second leading cause of mortality worldwide [1]. Based on data provided by the World Health Organization (WHO), it is projected that by the year 2030, there will be a total of 25 million newly diagnosed cases of cancer, resulting in approximately 10 million fatalities. Among the various types of cancer, breast, lung, colon, rectal, and prostate cancers are anticipated to exhibit the highest incidence rates [2, 3]. In this context, cancer presents a significant threat to human well-being and a significant challenge to the advancement of medical research in the development of innovative and efficacious anti-cancer drugs. Triazoles are nitrogen-containing heterocyclic compounds consisting of a five-membered ring of three nitrogen and two carbon atoms. Triazoles have been identified as efficacious bioisosteres of amides in bioactive compounds exhibiting a wide range of significant biological properties [4–7]. The 1,2,3-triazole heterocyclic system possess the capability to engage in hydrogen bond formation, dipole-dipole interactions, and π stacking interactions. Furthermore, it exhibit stability towards both reduction and oxidation [8]. 1,2,3-Triazole is commonly found in various therapeutic agents, such as tazobactam, carboxyamidotriazole, and Rufinamide, etc. The literature indicates that triazoles possess various pharmacological properties, including anticancer [9, 10], antitubercular [11], antifungal [12, 13], antibacterial [14, 15], antiviral [16, 17], antiobesity [18, 19], and anti-diabetic [20] activities. Thiadiazole is a prevalent and important five-membered heterocyclic system containing two nitrogen atoms and a sulfur atom. The presence of an amine group at the second position of the five-membered ring results in the formation of 2-aminothiadiazoles, which are commonly found in various drugs such as acetazolamide, megazol, cefazolin, etc. The thiadiazole amines exhibit a wide range of biological activities, including inhibition of Carbonic anhydrase (CA) [21], antibacterial [22], antifungal [23], anticancer [24, 25], antileishmanial [26], and anticonvulsant [27]. The motivation to develop a hybrid with strong anti-cancer activity stems from the observed anti-cancer properties of the 1,2,3-triazole and tetrazole scaffolds, as depicted in Fig. 1.

Considering the captivating characteristics of triazole, tetrazole, and thiadiazole as discussed in the existing literature, we have synthesized a novel set of twelve 1,2,3-triazole-thiadiazole hybrid compounds, which adhere to the scaffold depicted in Fig. 1. The cytotoxicity and apoptotic characteristics of the synthesized compounds were assessed in order to ascertain their potential as anti-cancer agents against human esophageal squamous cell carcinoma cells KYSE-450, which exhibit overexpression of Arora kinase A (ARK-A), and the pancreatic carcinoma cell line MIA PaCa-2, which exhibits overexpression of ERK2 (MIA PaCa-2). Subsequently, the derivatives exhibiting the highest potential within the series were subjected to in-vitro testing to evaluate their ability to inhibit kinase activity, specifically targeting both ARK-A and ERK2.

Results and discussion

Chemistry

The synthesis of target compounds 1-(5-(4-(diethylamino)-2-((1-phenyl-1H-1,2,3-triazol-4-yl)methoxy)phenyl)-1,3,4-thiadiazol-2-yl)pyrrolidine-2,5-dione (9a-l) is presented in Scheme 1. The intermediate compound of 2-(5-amino-1,3,4-thiadiazol-2-yl)-5-(diethylamino)phenol (3) was synthesized by reacting 4-(diethylamino)-2-hydroxybenzaldehyde (1) with thiosemicarbazide(2) in the presence of tert-butyl hydroperoxide (TBHP) in ethanol at room temperature for 4 h. This reaction resulted in the formation of 2-(5-amino-1,3,4-thiadiazol-2-yl)-5-(diethylamino)phenol (3) [28]. The amine compound (3) was protected using succinic anhydride (4) through a reflux process in water for 2.5 h, followed by being kept at room temperature overnight. This procedure resulted in the formation of an N-protected compound, specifically 1-(5-(4-(diethylamino)-2-hydroxyphenyl)-1,3,4-thiadiazol-2-yl)pyrrolidine-2,5-dione (5) [29]. The compound with a hydroxyl group (5) was subjected to propargylation using propargyl bromide (6) in the presence of dry K_2CO_3 in dry DMF. This reaction resulted in the formation of 1-(5-(4-(diethylamino)-2-(prop-2-ynyloxy)phenyl)-1,3,4-thiadiazol-2-yl)pyrrolidine-2,5-dione (7). Compound 7 undergoes subsequent reactions with substituted aryl azides(8a-l) to form triazoles through the utilization of click chemistry, resulting in the production of 1-(5-(4-(diethylamino)-2-((1-substitutedphenyl-1H-1,2,3-triazol-4-yl)methoxy)phenyl)-1,3,4-thiadiazol-2-yl)pyrrolidine-2,5-dione derivatives(9a-l). The products were obtained with yields ranging from 60% to 70% [30].

Cytotoxic evaluation

The newly synthesized hybrid molecules (**9a-l**) were screened against human esophageal squamous cell carcinoma cells KYSE-450 having ARK-A overexpression, human pancreatic carcinoma cells MIA PaCa-2 having ERK2 overexpression by using doxorubicin as a standard drug. The calculated IC_{50} values of all compounds are presented in Table 3. The compounds **9b, 9i**, and **9j** showed superior activity against KYSE-450 cells with

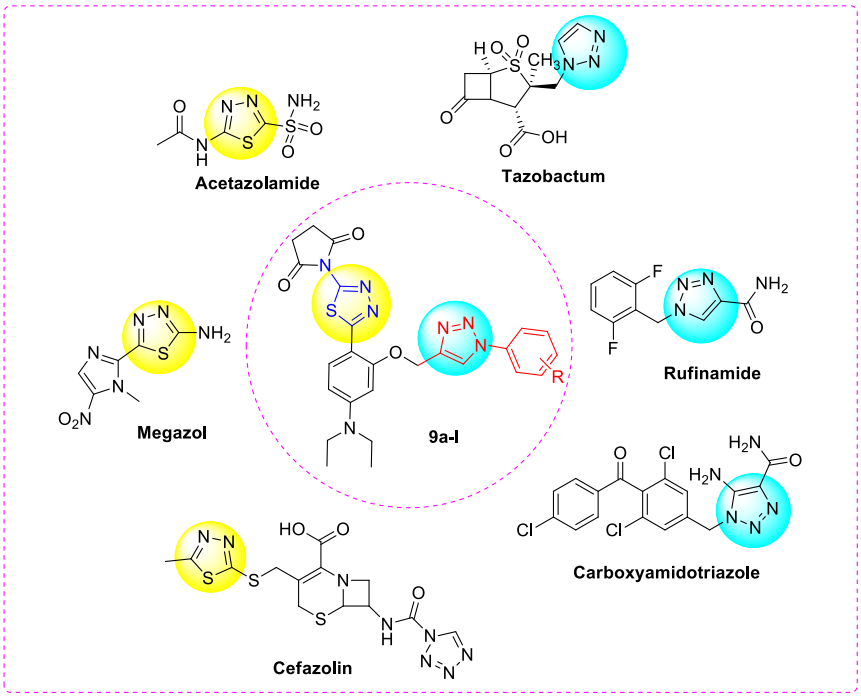

Fig. 1 The design rationale for the 1,2,3-triazole- thiadiazole hybrids

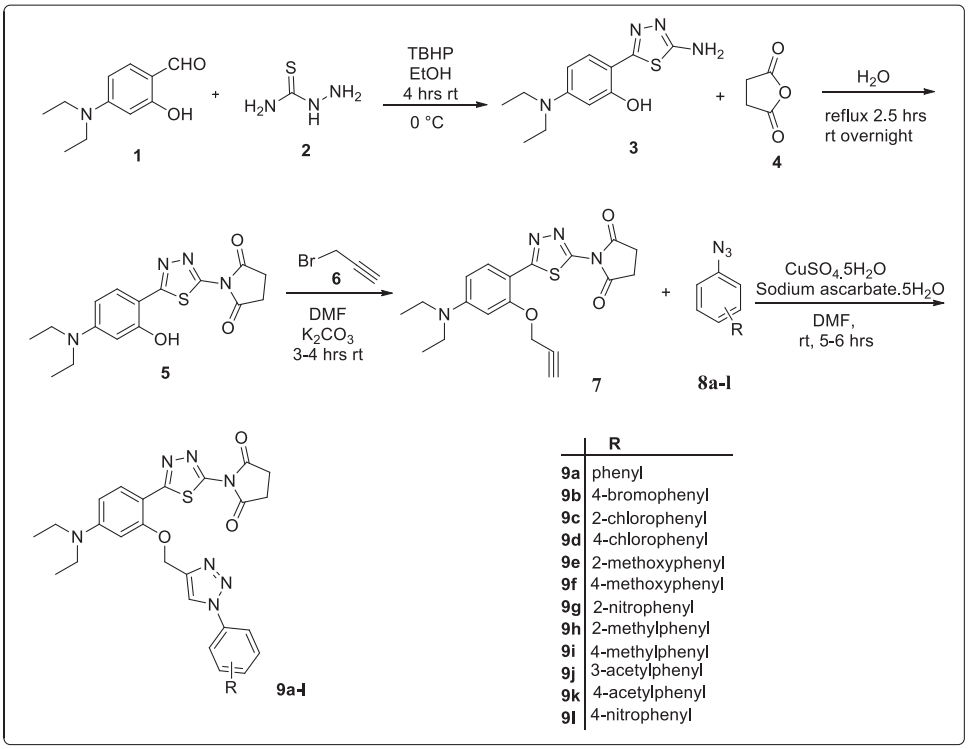

Scheme 1 Synthesis of 1-(5-(4-(diethylamino)-2-((1-substitutedphenyl-1H-1,2,3-triazol-4-yl)methoxy)phenyl)-1,3,4-thiadiazol-2-yl) pyrrolidine-2,5-dione derivatives (**9a-l**)

IC_{50} of 25.51 ± 1.38, 25.39 ± 1.35, and 23.74 ± 1.39 µM, respectively, than the standard drug doxorubicin. Although the three molecules mentioned above exhibit moderate to good cytotoxicity, compound **9j** demonstrated the lowest IC_{50}, suggesting slightly increased cytotoxic effects against KYSE-450 cells. On the other hand, compounds **9j** and **9l** showed promising cytotoxic activity against MIA PaCa-2 cells with IC_{50} of 20.62 ± 2.18 and 19.17 ± 1.16 µM, respectively. Both compounds showed superior cytotoxic behavior against MIA PaCa-2 cells. The remaining compounds failed to significantly affect the growth and proliferation of both KYSE-450 and MIA PaCa-2 cells. So these results demonstrated that compounds **9b, 9i**,

Table 1 Anti-cancer activity of the synthesized compounds (**9a-l**)

Compound Code	IC_{50} in μM	
	KYSE-450	MIA PaCa-2
9a	41.23 ± 1.4	36.59 ± 3.86
9b	**25.51 ± 1.38**	29.08 ± 2.04
9c	35.69 ± 1.76	33.13 ± 2.86
9d	50.17 ± 2.16	42.39 ± 3.04
9e	68.17 ± 3.25	41.75 ± 2.49
9f	30.60 ± 2.08	28.28 ± 2.29
9g	59.63 ± 4.63	40.16 ± 2.74
9h	74.31 ± 5.82	59.13 ± 3.91
9i	**25.39 ± 1.35**	22.93 ± 1.67
9j	**23.74 ± 1.39**	**20.62 ± 2.18**
9k	65.03 ± 6.08	62.17 ± 025
9l	46.28 ± 121.	**19.17 ± 1.16**
Doxorubicin	**27.06 ± 2.84**	**21.31 ± 0.83**

Bold values indicate the therapeutic significance of corresponding molecules

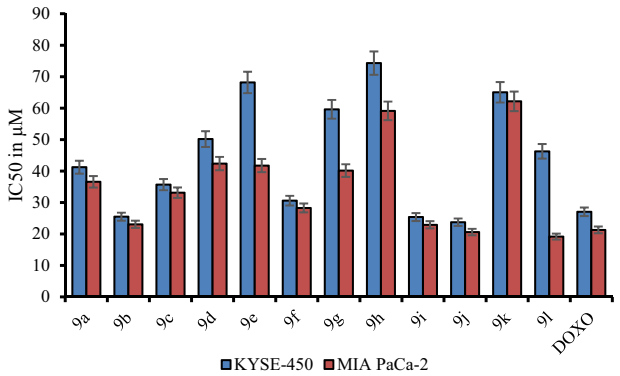

Fig. 2 IC_{50} of newly synthesized series (9a-l) against KYSE-450 and MIA PaCa cells

and **9j** demonstrated moderate to good cytotoxic behavior against both KYSE-450 and MIA PaCa-2 cells (Table 1 and Fig. 2). The observed activity of compounds **9b, 9i, 9j**, and **9l** can be attributed to the presence of either a weak electron-withdrawing group, such as bromine at the para position, or moderate to weak electron-donating functional groups, such as methoxy, methyl, and acetyl groups, at the meta or para positions.

Morphological observation

The cytotoxic effects of potent compounds (**9b, 9i, 9j**, and **9l**) were determined by observing morphological changes in KYSE-450 and MIA PaCa-2 cells. Compounds demonstrating cytotoxic effects commonly display characteristic features such as cellular shrinkage, membrane rounding, nuclear condensation, and the formation of vesicular structures within cells. The identification of morphological changes in cytotoxic cells through characteristic and typical morphological alterations was critically used to track changes during the course of therapy. Therefore, an inverted phase contrast microscope was used to observe the morphological changes. Following a 24 h exposure to test compounds, KYSE-450 and MIA PaCa-2 cells displayed discernible alterations in their morphology when compared to control cells, as depicted in Fig. 3. The examination of the control cells demonstrated that they maintained their initial morphology and architectural structure. In contrast, when subjected to specific compounds for a duration of 24 h, KYSE-450 and MIA PaCa-2 cells displayed typical cellular morphological changes, such as cellular rounding, shrinkage, and detachment from adjacent cells. Compound **9j** exhibited a significant impact on the cellular morphology of KYSE-450 and MIA PaCa-2 cells. Compounds **9b** and **9i** exhibited a significant impact on the cellular morphology of KYSE-450 cells, whereas compound **9l** elicited a similar effect on MIA PaCa cells Table 2.

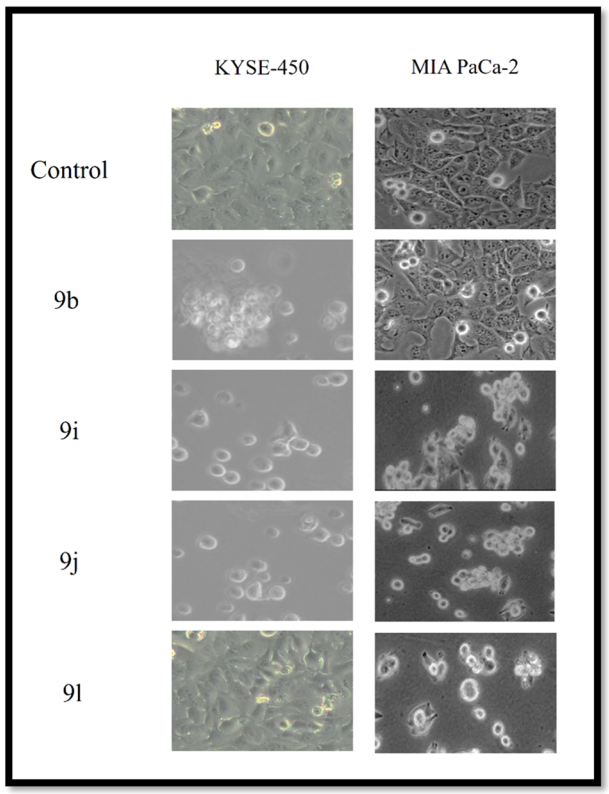

Fig. 3 Morphological examination of selected compounds (9b, 9i, 9j, and 9l)against KYSE-450 and MIA PaCa-2 cells

Dual kinase inhibition assay

The primary goal of synthesizing novel derivatives is to enhance the dual inhibition of ARK-A and ERK2, while

Table 2 Kinase inhibition of compounds 9a-l

Entry	Kinase inhibition in IC_{50} (μM)	
	ARK-A	ERK2
9a	>1	>1
9b	**0.034 ± 0.166**	0.256 ± 0.134
9c	0.749 ± 0.133	0.698 ± 0.135
9d	0.481 ± 0.095	0.593 ± 0.104
9e	0.251 ± 0.007	0.459 ± 0.115
9f	0.547 ± 0.096	0.689 ± 0.108
9g	0.531 ± 0.003	0.028 ± 0.002
9h	0.813 ± 0.159	0.782 ± 0.186
9i	0.124 ± 0.166	**0.024 ± 0.192**
9j	**0.018 ± 0.135**	**0.017 ± 0.124**
9k	0.486 ± 0.116	0.509 ± 0.137
9l	0.047 ± 0.007	0.031 ± 0.003
Barasertib	**0.021 ± 0.007**	-
Temuterkib	-	**0.019 ± 0.003**

Bold values indicate the therapeutic significance of corresponding molecules

simultaneously mitigating their toxic effects. Therefore, the inhibition of ARK-A/ERK2 kinase was employed to assess in vitro enzymatic inhibitory studies that ultimately reflect the anti-tumor properties of the developed agents. The inhibition of the ARK-A/ERK2 kinase was carried out in accordance with the instructions provided by the developers of the commercial assay kits. As illustrated in Table 4, it was observed that out of the twelve synthesized compounds, only one **(9j)** displayed significant inhibitory activity against ARK-A and ERK2. This finding suggests that the strategic design of the compound's structure played a role in its observed activity. Compound **9j** from the series exhibited more pronounced inhibition of both ARK-A/ERK2 inhibitory activities, as evidenced by IC_{50} values of 0.018 ± 0.13 and 0.017 ± 0.124 μM, respectively. Compound **9b** exhibited potent inhibitory activity against ARK-A, with an IC_{50} value of 0.034 ± 0.166 μM. Similarly, compound **9l** demonstrated notable activity against ERK-2, with an IC_{50} value of 0.024 ± 0.192 μM. The findings of this study further support the cytotoxic activity of these compounds, as evidenced by their anti-proliferative properties.

Molecular Docking with Aurora-related Kinase A

The ligands exhibit greater binding affinities towards Aurora kinase A (PDB ID: 1MQ4) in comparison to the standard reference compound, doxorubicin. The docking scores of compounds **9a-l** exhibit a range spanning from −9.8 to −10.5 Kcal/mol, surpassing the value of −9.8 Kcal/mol observed for Doxorubicin (Table 3). The active site pocket of Aurora kinase A was identified by the CASTp server to

Table 3 The binding energies and interactions of synthesized molecules with Aurora related kinase A (PDB ID: 1MQ4)

Compounds	Binding Energy (Kcal/mol)	Interacting amino acids	
		H-bond	hydrophobic
9a	−10.0	Lys143, Asp256, Asn261	Leu139, Val147, Ala160, Lys162, Ala213, Tyr219, Glu260, Leu263, Asp274
9b	−10.0	Asp256, Asn261, Trp277	Leu139, Lys143, Val147, Ala160, Lys162, Tyr212, Ala213, Leu263, Asp274
9c	−10.3	Asp256, Asn261, Trp277	Leu139, Lys143, Val147, Ala160, Lys162, Tyr212, Ala213, Leu263, Asp274
9d	−10.3	Asp256, Asn261, Trp277	Leu139, Lys143, Val147, Ala160, Lys162, Tyr212, Ala213, Leu263, Asp274
9e	−10.3	Lys143, Lys162, Asn261	Leu139, Lys141, Lys143, Val147, Ala160, Lys162, Ala213, Tyr219, Leu263, Asp274
9f	−9.8	Asp256, Glu260, Asn261, Trp277	Leu139, Lys143, Val147, Ala160, Lys258, Leu263, Asp274
9g	−9.9	Lys162, Gln177, Asp256, Asn261, Asp274	Leu139, Phe144, Val147, Ala160, Ala213, Asn261, Leu263, Asp277
9h	−10.2	Asp256, Glu260, Asn261, Asp274	Leu139, Lys143, Val147, Ala160, Glu260, Leu263, Asp274
9i	−10.4	Asp256, Asn261	Leu139, Lys143, Val147, Ala160, Lys162, Tyr212, Ala213, Leu263, Asp274, Trp277
9j	−10.4	Lys162, Asp256, Asn261	Leu139, Lys143, Val147, Ala160, Lys162, Ala213, Tyr219, Glu260, Leu263, Asp274
9k	−10.5	Lys141, Lys162, Ala213	Leu139, Lys143, Phe144, Val147, Lys162, Glu181, Leu263, Asp274
9l	−10.3	Ala213, Asp256, Asn261, Trp277	Leu139, Lys143, Val147, Ala160, Lys162, Leu263, Asp274
Doxorubicin	−9.8	Lys143, Glu260, Asn261, Asp274	Leu139, Lys141, Gly142, Val147, Ala160, Ala213, Leu263

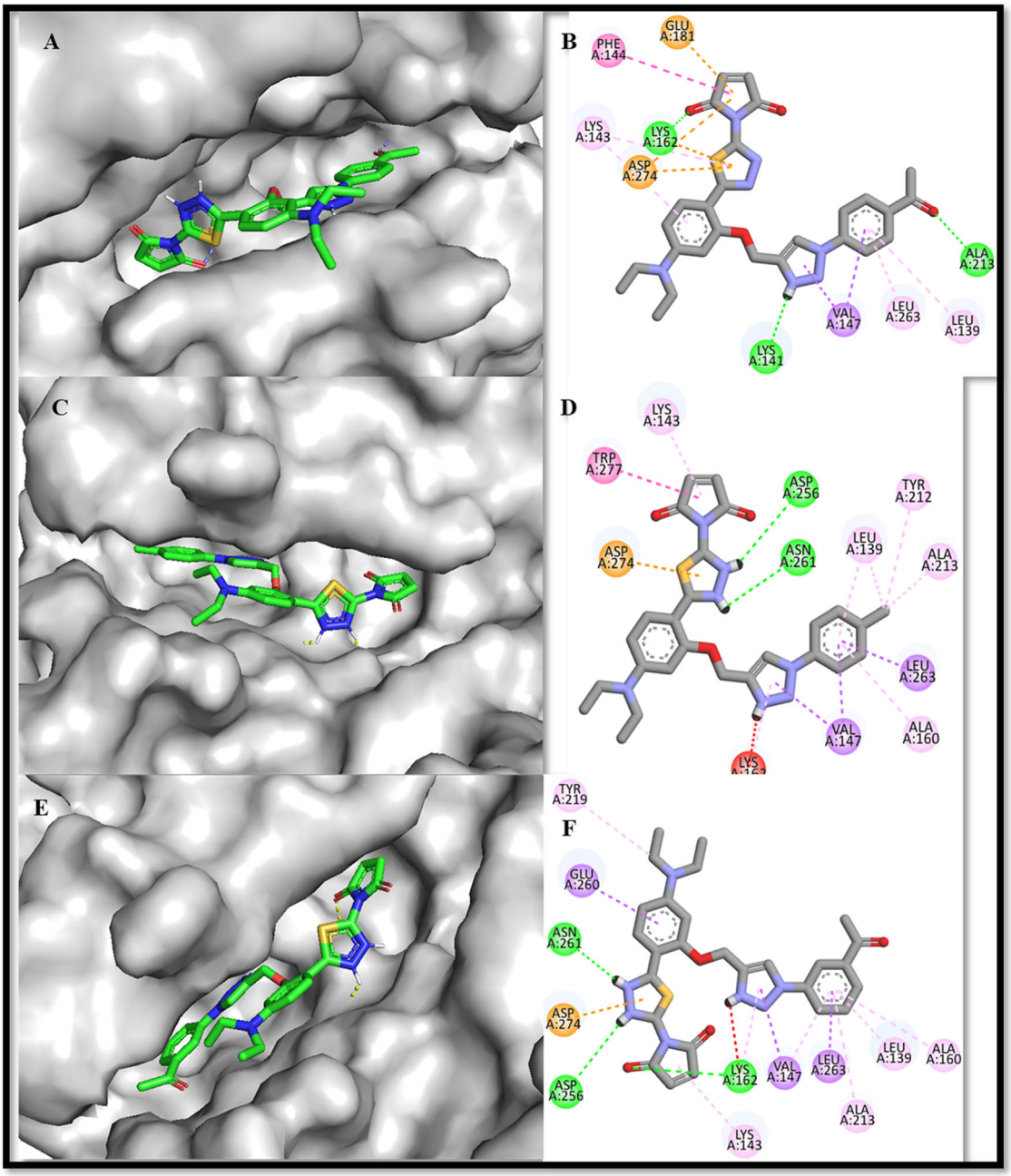

Fig. 4 **A** 3D and (**B**) 2D Docking pose of compound **9k** in the cavity of 1MQ4; **C** 3D and (**D**)2D Docking pose of compound **9i** in the cavity of 1MQ4; **E** 3D and **F**)2D Docking pose of compound **9j** in the cavity of 1MQ4

contain the following amino acids: Leu139, Gly140, Lys141, Gly142, Lys143, Val147, Ala160, Lys162, His176, Arg180, Leu194, Glu211, Ala213, Thr217, Arg255, Glu260, Asn261, Leu263, Asn277, Trp277, Ser284, Arg285, and Thr292. The novel ligand molecules have exhibited notable interactions, encompassing electrostatic or salt bridge interactions, with crucial residues such as Lys141, Lys143, Lys162, Asp256, and Asp277. Moreover, the ligands in question establish hydrogen bonding interactions with Gln177, Ala213, and Asp256, and also demonstrate π-π stacking interactions with Trp277 within the active sites of Arora kinase-A. Compound **9k** demonstrated the most pronounced binding affinity with -10.5 Kcal/mol. The compound demonstrated significant interactions with amino acid residues Lys141, Lys162, and Ala213, as well as hydrophobic interactions with Leu139, Lys143, Phe144, Val147, Lys162, Glu181, Leu263, and Asp274 of the protein structure 1MQ4 (Fig. 4A, B). Compounds **9i** and **9j** exhibited the second-highest level of binding

Table 4 The binding energies and interactions of synthesized molecules with extracellular signal-related kinase 2 (PDB ID: 4ZXT)

Compounds	Binding Energy (Kcal/mol)	Interacting amino acids	
		H-bond	hydrophobic
9a	−8.8	Gln105, Asp111, Lys114, Ser153	Ile31, Ala35, Tyr36, Val39, Ala52, Lys54, Ileu156, Asp167
9b	−8.3	Gln105, Asp111, Lys114, Ser153	Ile31, Ala35, Tyr36, Val39, Ala52, Lys54, Asp111, Lys114, Leu156, Asp167
9c	−8.2	Lys54, Asn154	Gly34, Ala35, Tyr36, Arg67, Ile84, Lys114, Leu156, Asp167
9d	−8.5	Gln105, Asp111, Lys114, Ser153	Ile31, Ala35, Tyr36, Val39, Ala52, Lys54, Asp111, Lys114, Asp167
9e	−8.8	Gln105, Asp111, Lys114, Ser153	Ala35, Tyr36, Val39, Ala52, Lys54, Asp111, Lys114, Leu156, Asp167
9f	−8.4	Asp111, Lys114, Ser153	Ile31, Ala35, Tyr36, Val39, Ala52, Lys54, Asp111, Lys114, Leu156, Asp167
9g	−8.2	Gln105, Asp111, Lys114, Ser153	Ile31, Ala35, Tyr36, Val39, Lys54, Asp111, Leu156, Asp167
9h	−9.0	Asp111, Lys114, Ser153	Ile31, Ala35, Tyr36, Val39, Lys54, Asp111, Lys114, Leu156, Asp167
9i	−8.5	Gln105, Asp111, Lys114, Ser153	Ile31, Ala35, Tyr36, Val39, Ala52, Lys54, Asp111, Lys114, Leu156, Asp167
9j	−9.3	Tyr39, Arg67, Lys151, Ser153, Asn154	Ala35, Val39, Lys54, Arg67, Lys151, Leu156, Asp167
9k	−8.2	Glu33, Met108, Asp111	Ile31, Val36, Val39, Ala52, Leu156
9l	−8.7	Gln105, Asp111, Lys114, Ser153	Ile31, Ala35, Tyr36, Val39, Ala52, Lys54, Asp111, Lys114, Leu156, Asp167
Doxorubicin	−8.3	Lys54, Gln105, Asp111, Lys114	Ile31, Gly34, Ala35, Tyr36, Asp111, Ser153, Asp167

affinity, with a value of −10.4 Kcal/mol. Compound **9i** exhibited notable interactions with Asp256 and Asn261, whereas compound **9j** displayed substantial interactions with Lys162, Asp256, and Asn261. Figure 4C–F illustrates the hydrogen bonding and hydrophobic interactions observed for compounds **9i** and **9j**.

Molecular docking with extracellular signal-related kinase 2 (ERK2)

The synthesized ligand molecules demonstrated binding energies that were similar to those of the widely accepted reference compound doxorubicin when they interacted with ERK2 (PDB ID: 4ZXT). The compounds **8a - 8l** exhibited docking scores ranging from −8.2 to −9.3 Kcal/mol, while doxorubicin demonstrates a docking score of −8.3 Kcal/mol. According to Table 4, The active site pocket of ERK2 is composed of specific amino acids, namely Ile31, Gly32, Glu33, Gly34, Ala35, Tyr36, Gly37, Met38, Val39, Ala52, Lys54, Lys55, Ile56, Arg67, Thr68, Glu71, Ile72, Leu75, Ile84, Ile103, Gln105, Asp106, Leu107, Met108, Glu109, Thr110, Asp111, Lys114, Asp149, Lys151, Ser153, Asn154, Leu156, Ile165, Asp167, Gly169, and Leu170. These amino acids were determined using the CASTp server. The novel ligand molecules have demonstrated significant interactions with the active sites Glu33, Tyr39, Lys54, Arg67, Gln105, Met108, Asp111, Lys114, Ser153, and Asn154 of ERK2.

Compound **9j** exhibited the most notable binding affinity with a value of −9.3 Kcal/mol. The compound demonstrated hydrogen bonding interactions with Tyr39, Arg67, Lys151, Ser153, Asn154, as well as hydrophobic interactions with Ala35, Val39, Lys54, Arg67, Lys151, Leu156, and Asp167 of ERK2, as depicted in Fig. 5A, B. The interactions of **9h** with 4ZXT (Fig. 5C, D) were characterized by its key interactions with Asp111, Lys114, Ser153, as well as hydrophobic interactions involving Ile31, Ala35, Tyr36, Val39, Lys54, Asp111, Lys114, Leu156, and Asp167.

Conclusion

Fused heterocyclic ring systems have attracted significant attention as promising candidates for cancer therapy. In recent studies, it has been demonstrated that derivatives of imidazothiadiazol-yl)-1H-Indole exhibit promising potential as therapeutic agents for the treatment of pancreatic cancer [28]. In the present work, a new series of molecular hybrids containing 1,2,3-triazole and thiazolidinediones were synthesized and evaluated for their anti-cancer activity against human esophageal carcinoma cell lines KYSE-450 and human pancreatic carcinoma cell line MIA PaCa-2 cells. Docking studies revealed that 9k, 9j, and 9i showed significant docking scores with the ARK-A receptor, indicating

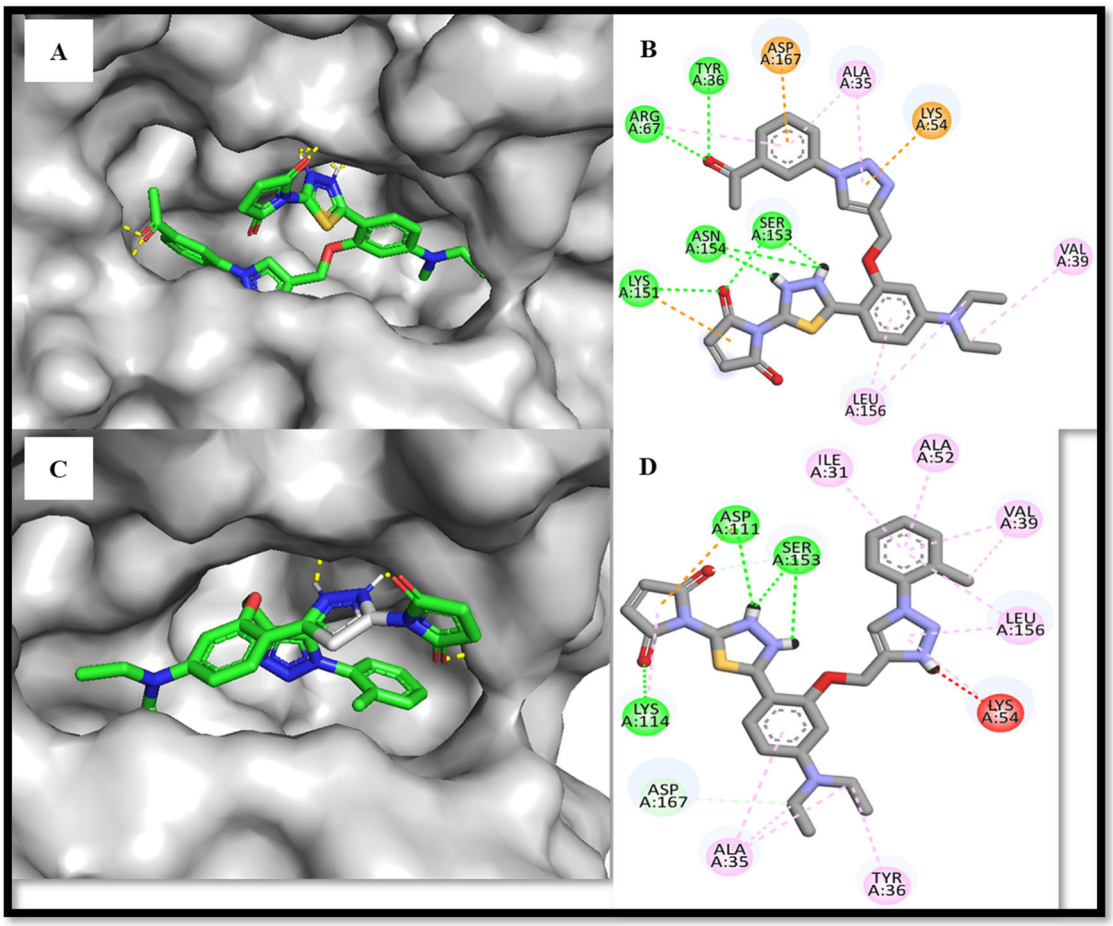

Fig. 5 **A** 3D and (**B**) 2D Docking pose of compound **9j** in the cavity of 4ZXT; (**C**) 3D and (**D**) 2D Docking pose of compound **9h** in the cavity of 4ZXT

strong binding interactions. Molecules 9j and 9 h exhibited significant binding interactions with the ERK-2 receptor indicating inhibitory activity. Cytotoxic data examined that compounds 9b, 9i, 9j, and 9 l showed promising activity against KYSE-450 and MIA PaCa-2 cells. Among all compounds tested, compound 9j showed superior anti-cancer potential compared to the standards. The other compounds showed moderate to weak activities against the cell lines. Further, Kinase inhibition of compound 9j showed a substantially higher effect against ARK-A and ERK-2 enzymes in-vitro. The synthesized compounds are better lead compounds for developing new anti-cancer agents.

Experimental

General experimental methods

Unless specified, all the chemicals and solvents were purchased from commercial vendors and used for further purification. ^{1}H NMR and ^{13}C NMR spectra were recorded in DMSO using 500 MHz spectrometers (Bruker Avance III 500 MHz). Chemical shift values are displayed as ppm, and spin multiplicities are indicated as singlet (s); doublet (d); doublet of doublet (dd); triplet(t); multiplets (m); and coupling constants are shown in hertz. Column chromatography was performed on silica gel (60–120 mesh) using distilled hexane and ethyl acetate solvents. Mass and Infrared spectra were recorded on QSTAR XL GCMS, Perkin Elmer spectrum-2 mass spectrometer. Melting points were determined in an open glass capillary tube on a Stuart MP2. Melting Point apparatus and were uncorrected.

Synthesis of 2-(5-amino-1,3,4-thiadiazol-2-yl)-5-(diethylamino)phenol **(3)**: The compound 4-(diethylamino)-2-hydroxybenzaldehyde **(1)** was dissolved in ethanol and combined with thiosemicarbazide**(2)** at room temperature. The resulting mixture was stirred for 2 h. Subsequently, the reaction mixture was cooled to a temperature of 0–5 °C, and tert-butyl hydroperoxide (TBHP) was gradually introduced to the reaction under inert conditions. The reaction was then allowed to continue stirring for an additional 35 h. Upon the

completion of the reaction, the solvent was evaporated, and the resulting residue was combined with crushed ice. The mixture was subjected to three extractions using 100 mL of ethyl acetate each time. The resulting solution was then dried using anhydrous sodium sulfate and subsequently evaporated under reduced pressure. This process yielded 2-(5-amino-1,3,4-thiadiazol-2-yl)-5-(diethylamino) phenol **(3)** with a 60% yield [28].

Synthesis of 1-(5-(4-(diethylamino)-2-hydroxyphenyl)-1,3,4-thiadiazol-2-yl)pyrrolidine-2,5-dione **(5)**: The compound 2-(5-amino-1,3,4-thiadiazol-2-yl)-5-(diethylamino) phenol **(3)** was subjected to amine protection using succinic anhydride **(4)** in a reflux setup with water for a duration of 2.5 h. The reaction mixture was then allowed to stand at room temperature overnight to yield the desired product [29].

Synthesis of 1-(5-(4-(diethylamino)-2-(prop-2-ynyloxy) phenyl)-1,3,4-thiadiazol-2-yl)pyrrolidine-2,5-dione **(7)**: The reaction involved the addition of a mixture of compound **5** and dry K_2CO_3 in dry DMF to propargyl bromide **(6)**, followed by stirring for 4 h. The progress of the reaction was assessed through TLC. Upon completion, the reaction mixture was transferred into crushed ice and vigorously agitated. The resulting precipitate was subsequently filtered to yield 1-(5-(4-(diethylamino)-2-(prop-2-ynyloxy)phenyl)-1,3,4-thiadiazol-2-yl) pyrrolidine-2,5-dione **(7)**, and was purified using column chromatography with eluaenr of ethyl acetate and hexane in a ratio of 4:6.

General procedure for the synthesis of 1-(5-(4-(diethylamino)-2-((1-phenyl-1*H*-1,2,3-triazol-4-yl)methoxy)phenyl)-1,3,4-thiadiazol-2-yl)pyrrolidine-2,5-dione hybrids **(9a-l)**: To a solution of compound **(7)** (0.1 mmol) and appropriate aryl azides**(8a-l)** (0.15 mmol) in DMF: H_2O was added $CuSO_4.5H_2O$ (3 mol%) with sodium ascorbate (5 mol%) and stirred at room temperature for 6–8 h. TLC monitored the completion of the reaction. Upon completion of the reaction, mass was purified by column chromatography using hexane/ ethyl acetate (1:3) to afford titled compounds (**9a-l**)with good yields of 60–70% [30].

Anti-cancer activity

Cellular Cytotoxicity Assays

Esophageal squamous cell carcinoma with ARK-A overexpression (KYSE-450), Pancreatic carcinoma cell line with ERK2 overexpression (MIA PaCa-2)were provided by the Center for Cellular and Molecular Biology (CCMB), Hyderabad, India. Cells were cultured in RPMI 1640 medium supplemented with 10% FBS, and Penicillin 100 U/mL and Streptomycin 100 U/mL were added. Cell cultures were maintained in a humidified atmosphere of 5% CO_2 at 37 °C. Cells were seeded at respective densities (2.5×10^4 /mL) in 96-well plates in a volume of 180 µL per well. After seeding for 24 h, the medium was removed. The test compounds were dissolved in DMSO and diluted with a culture medium to different concentrations (the final concentration of DMSO was 0.1%). Then, 20 µL of the test compound solution **(9a-l)**was added in duplicates, and incubation continued for 48 h in a humidified atmosphere of 5% CO_2 at 37 °C. After removing the medium, 20 µLof methyl thiazolyl diphenyl-tetrazolium bromide (MTT) was added to each well and incubated for 3–4 h. The growth medium was replaced by 150 µL DMSO to solubilize the purple formazan crystals produced, and the absorbance was measured on a microplate reader at 570 nm. The compound IC_{50} values were calculated using Graph Pad Prism 5.0. Data represented as mean ± SD from three independent experiments.

Morphological Observation using Phase contrast microscopy

Observation of morphological changes of cytotoxic effect was performed according to the method with slight modifications. Briefly, 5×10^5 cells were incubated for 48 h with or without selected compounds (**9b**, **9i**, **9j**, and 9l) at double IC_{50} concentrations in 60 mm diameter tissue culture dishes. The medium was discarded, and cells were washed once with PBS. The morphological changes of the cytotoxic effect over the treatment were observed using a phase contrast inverted microscope (Leica DMI 3000B, Germany) at 200x magnifications.

Kinase inhibitory assays

Selectivity screening of newly synthesized compounds (**9a-l**)against aurora kinase A (ARK-A) and extracellular regulated kinase 1 (ERK1) kinases was performed by using PromegaADP-Glo™ bioluminescent detection of kinase assay kit as per the manufacturer's guidelines. Two kinases, ARK-A and ERK1, were used in multipoint dose-response experiments. The kinase and substrate strips were diluted in 45 µL of 5x kinase buffer solution and 7.5 µL of 200 µM ATP, respectively. Kinase reactions were performed using 1 µL of the compound solution at varying concentrations (0.05–50 µM), 3 µL of kinase working stock, and 3 µL of ATP/substrate working stock. After 1 h incubation at room temperature, kinase activity was quantified using the ADP-Glo Kinase Assay (Promega Corporation, Madison, WI, USA). Kinase inhibition was quantified using a luminescence microplate spectrophotometer Infinitive M1000 (Tecan, Groding, Austria). The concentration of the test compounds required to decrease the kinase activity by 50% was determined using ImageJ software and identified as the IC_{50}. This study measures the quantitative behavior of ARK-A/ERK2 inhibition.

Molecular docking studies

Molecular docking is a reliable, cost-effective, and time-saving technique in drug discovery [31]. AutodockVina of PyRx tool is an open-source software tool [32] used for performing docking studies. AutodockVina uses an empirical scoring function to calculate the binding affinity of the protein-ligand complex [33]. For a better understanding of the binding interactions between ligand molecules and target cancer cells, the crystal structure of the breast cancer drug target aurora-related kinase A (PDB ID: **1MQ4**) [34] and lung cancer target extracellular signal-related kinase 2 (ERK2) (PDB ID: **4ZXT**) [35] were retrieved from Protein Data Bank (www.rcsb.org). The proteins were prepared by using the Biovia Discovery Studio software tool. Initially, water molecules were removed, and polar hydrogens were added to a macromolecule. The ligands were sketched using the Chemsketch tool (www.acdlabs.com) and saved in MDL file format. Both target and ligand molecules were loaded into the PyRx tool. The energies of ligands were minimized and converted to PDBQT file format. The protein was chosen as a macromolecule. The active site pockets of target molecules were determined by CASTp online server [36, 37]. The 3D grid box was set up in such a way as to cover the active site pocket of the target molecule and docking simulations were performed. After docking, conformations were ranked according to their binding energy, and the confirmation with the lowest binding energy was considered the best docking score. The docking results were visualized using PyMOL and Biovia Discovery Studio Visualizer.

Spectral data of Target compounds

2-(5-(4-(diethylamino)-2-((1-phenyl-1H-1,2,3-triazol-4-yl)methoxy)phenyl)-1,3,4-thiadiazol-2-yl)cyclopentane-1,3-dione **(9a)**: Yield 60%, mp: 124–126 °C; Rf = 0.34 (EtOAc: n-Hexane 2:3);^{1}H NMR (500 MHz, DMSO-d_6) δ 8.55 (s, 1H), 7.73 (d, J = 7.6 Hz, 1H), 7.59–7.53 (m, 2H), 7.52–7.44 (m, 2H), 7.42–7.35 (m, 1H), 6.78 (d, J = 2.3 Hz, 1H), 6.52 (s, 1H), 5.38 (s, 2H), 3.47 (q, J = 7.0 Hz, 4H), 2.71 (s, 4H), 1.12 (t, J = 7.0 Hz, 6H); ^{13}C NMR (125 MHz, DMSO-d_6) δ 174.10, 157.78, 156.66, 153.41, 150.82, 146.25, 135.72, 129.36, 129.19, 126.91, 120.13, 119.15, 114.14, 106.52, 98.39, 58.57, 43.83, 28.14, 11.66. LC-MS $[M + H]^+$; 502.59: Elemental analysis, Calculated, %: $C_{26}H_{26}N_6O_3S$: C, 62.13; H, 5.21; N, 16.72; Found %: C, 62.08; H, 5.16; N, 16.68;

2-(5-(2-((1-(4-bromophenyl)-1H-1,2,3-triazol-4-yl)methoxy)-4-(diethylamino)phenyl)-1,3,4-thiadiazol-2-yl)cyclopentane-1,3-dione **(9b)**: Yield 63%, mp: 121–123 °C; Rf = 0.42 (EtOAc:n-Hexane 2:3); ^{1}H NMR (500 MHz, DMSO-d_6) δ 8.55 (s, 1H), 7.73 (d, J = 7.6 Hz, 1H), 7.70–7.58 (m, 4H), 6.78 (d, J = 2.3 Hz, 1H), 6.52 (s, 1H), 5.38 (s, 2H), 3.47 (q, J = 7.0 Hz, 4H), 2.71 (s, 4H), 1.12 (t, J = 7.0 Hz, 6H); ^{13}C NMR (125 MHz, DMSO-d_6) δ 174.14, 157.82, 156.70, 153.45, 150.86, 146.29, 134.53, 133.05, 129.23, 120.91, 119.22, 119.06, 114.18, 106.56, 98.43, 58.61, 43.87, 28.18, 11.70: LC-MS $[M + H]^+$; 581.48 Elemental analysis, Calculated, %: $C_{26}H_{25}BrN_6O_3S$:C,53.70; H, 4.33; N, 14.45; Found %: C,53.67; H, 4.31; N, 14.41

2-(5-(2-((1-(2-chlorophenyl)-1H-1,2,3-triazol-4-yl)methoxy)-4-(diethylamino)phenyl)-1,3,4-thiadiazol-2-yl)cyclopentane-1,3-dione **(9c)**: Yield 61%, mp: 127–129 °C; Rf = 0.40 (EtOAc: n-Hexane 2:3); ^{1}H NMR (500 MHz, DMSO-d_6) δ 8.46 (s, 1H), 7.79–7.71 (m, 2H), 7.52–7.44 (m, 2H), 7.37 (dd, J = 7.0, 1.3 Hz, 1H), 6.78 (d, J = 2.3 Hz, 1H), 6.52 (s, 1H), 5.37 (s, 2H), 3.47 (q, J = 7.0 Hz, 4H), 2.71 (s, 4H), 1.12 (t, J = 7.0 Hz, 6H); ^{13}C NMR (125 MHz, DMSO-d_6) δ 174.13, 157.81, 156.69, 153.44, 150.85, 145.82, 135.02, 130.96, 129.22, 128.19, 127.53, 127.13, 120.42, 119.22, 114.17, 106.55, 98.42, 58.77, 43.86, 28.17, 11.69. LC-MS $[M + H]^+$; 537.03: Elemental analysis, Calculated, %: $C_{26}H_{25}ClN_6O_3S$: C, 58.15; H, 4.69; N, 15.65; Found %: C, 58.11; H, 4.64; N, 15.61;

2-(5-(2-((1-(4-chlorophenyl)-1H-1,2,3-triazol-4-yl)methoxy)-4-(diethylamino)phenyl)-1,3,4-thiadiazol-2-yl)cyclopentane-1,3-dione **(9d)**: Yield 65%, mp: 129–131 °C; Rf = 0.40 (EtOAc: n-Hexane 2:3); ^{1}H NMR (500 MHz, DMSO-d_6) δ 8.55 (s, 1H), 7.76–7.70 (m, 3H), 7.48–7.42 (m, 2H), 6.78 (d, J = 2.3 Hz, 1H), 6.52 (s, 1H), 5.38 (s, 2H), 3.47 (q, J = 7.0 Hz, 4H), 2.71 (s, 4H), 1.12 (t, J = 7.0 Hz, 6H); ^{13}C NMR (125 MHz, DMSO-d_6) δ 174.10, 157.78, 156.66, 153.41, 150.82, 146.25, 134.17, 134.06, 129.65, 129.19, 121.52, 119.14, 114.14, 106.52, 98.39, 58.57, 43.83, 28.14, 11.66. LC-MS $[M + H]^+$; 537.03 Elemental analysis, Calculated, %: $C_{26}H_{25}ClN_6O_3S$: C, 58.15; H, 4.69; N, 15.65; Found %: C, 58.11; H, 4.64; N, 15.61;

2-(5-(4-(diethylamino)-2-((1-(4-hydroxyphenyl)-1H-1,2,3-triazol-4-yl)methoxy)phenyl)-1,3,4-thiadiazol-2-yl) cyclopentane-1,3-dione **(9e)**: Yield 60%, mp: 127–129 °C; Rf = 0.30 (EtOAc: n-Hexane 2:3); ^{1}H NMR (500 MHz, DMSO-d_6) δ 9.12 (s, 1H), 8.54 (s, 1H), 7.76–7.66 (m, 3H), 6.97–6.90 (m, 2H), 6.78 (d, J = 2.3 Hz, 1H), 6.52 (s, 1H), 5.38 (s, 2H), 3.47 (q, J = 7.0 Hz, 4H), 2.71 (s, 4H), 1.12 (t, J = 7.0 Hz, 6H); ^{13}C NMR (125 MHz, DMSO-d_6) δ 174.14, 157.82, 156.70, 156.14, 153.45, 150.86, 146.28, 129.23, 129.00, 121.41, 119.55, 116.77, 114.18, 106.56, 98.43, 58.61, 43.87, 28.18, 11.70. LC-MS $[M + H]^+$; 518.59: Elemental analysis, Calculated, %: $C_{26}H_{26}N_6O_4S$: C, 60.22; H, 5.05; N, 16.21; Found %: C, 60.18; H, 5.01; N, 16.17;

2-(5-(4-(diethylamino)-2-((1-(2-methoxyphenyl)-1H-1,2,3-triazol-4-yl)methoxy)phenyl)-1,3,4-thiadiazol-2-yl) cyclopentane-1,3-dione **(9f)**: Yield 62%, mp: 121–123 °C; Rf = 0.44 (EtOAc: n-Hexane 2:3); ^{1}H NMR (500 MHz, DMSO-d_6) δ 8.44 (s, 1H), 7.76–7.69 (m, 2H), 7.40 (dd, J = 7.1, 1.1 Hz, 1H), 7.18 (dd, J = 7.1, 1.4 Hz, 1H), 7.05 (d, J = 1.3 Hz, 1H), 6.78 (d, J = 2.3 Hz, 1H), 6.52 (s, 1H), 5.38

(s, 2H), 3.84 (s, 3H), 3.47 (q, $J = 7.0$ Hz, 6H), 2.71 (s, 4H), 1.12 (t, $J = 7.0$ Hz, 6H); ^{13}C NMR (125 MHz, DMSO-d_6) δ 174.12, 157.80, 156.68, 153.43, 153.19, 150.84, 145.26, 129.21, 127.97, 126.20, 124.21, 119.25, 119.06, 114.16, 113.38, 106.54, 98.41, 58.76, 55.06, 43.85, 28.16, 11.68. LC-MS $[M + H]^+$; 532.61: Elemental analysis, Calculated,%:: $C_{27}H_{28}N_6O_4S$: C, 60.89; H, 5.30; N, 15.78; Found %: C, 60.84; H, 5.26; N, 15.73;

2-(5-(4-(diethylamino)-2-((1-(4-methoxyphenyl)-1H-1,2,3-triazol-4-yl)methoxy)phenyl)-1,3,4-thiadiazol-2-yl) cyclopentane-1,3-dione **(9g)**: Yield 67%, mp: 126–128 °C; Rf = 0.44 (EtOAc: n-Hexane 2:3); ^{1}H NMR (500 MHz, DMSO-d_6) δ 8.53 (s, 1H), 7.73 (d, $J = 7.6$ Hz, 1H), 7.66–7.59 (m, 2H), 7.06–6.99 (m, 2H), 6.78 (d, $J = 2.3$ Hz, 1H), 6.52 (s, 1H), 5.38 (s, 2H), 3.76 (s, 3H), 3.47 (q, $J = 7.0$ Hz, 6H), 2.71 (s, 4H), 1.12 (t, $J = 7.0$ Hz, 6H); ^{13}C NMR (125 MHz, DMSO-d_6) δ 174.06, 159.15, 157.74, 156.62, 153.37, 150.78, 146.20, 130.05, 129.15, 121.39, 119.47, 114.62, 114.10, 106.48, 98.35, 58.53, 54.62, 43.79, 28.10, 11.62: LC-MS $[M + H]^+$; 532. Elemental analysis, Calculated,%: $C_{27}H_{28}N_6O_4S$: C, 60.89; H, 5.30; N, 15.78; Found %: C, 60.84; H, 5.26; N, 15.73;

2-(5-(4-(diethylamino)-2-((1-(o-tolyl)-1H-1,2,3-triazol-4-yl)methoxy)phenyl)-1,3,4-thiadiazol-2-yl)cyclopentane-1,3-dione **(9h)**: Yield 61%, mp: 119–121 °C; Rf = 0.45 (EtOAc: n-Hexane 2:3); ^{1}H NMR (500 MHz, DMSO-d_6) δ 8.57 (s, 1H), 7.73 (d, $J = 7.6$ Hz, 1H), 7.69 (d, $J = 1.4$ Hz, 1H), 7.41 (dd, $J = 7.1$, 1.4 Hz, 1H), 7.29–7.19 (m, 2H), 6.78 (d, $J = 2.3$ Hz, 1H), 6.52 (s, 1H), 5.38 (s, 2H), 3.47 (q, $J = 7.0$ Hz, 6H), 2.71 (s, 4H), 2.32 (s, 3H), 1.12 (t, $J = 7.0$ Hz, 6H); ^{13}C NMR (125 MHz, DMSO-d_6) δ 174.12, 157.80, 156.68, 153.43, 150.84, 145.86, 135.89, 132.10, 130.34, 129.21, 127.92, 126.79, 119.97, 119.08, 114.16, 106.54, 98.41, 58.76, 43.85, 28.16, 16.84, 11.68. LC-MS $[M + H]^+$; 516.61: Elemental analysis, Calculated,%: $C_{27}H_{28}N_6O_3S$: C, 62.77; H, 5.46; N, 16.27; Found %: C, 62.73; H, 5.42; N, 16.24;

2-(5-(4-(diethylamino)-2-((1-(p-tolyl)-1H-1,2,3-triazol-4-yl)methoxy)phenyl)-1,3,4-thiadiazol-2-yl)cyclopentane-1,3-dione **(9i)**: Yield 64%, mp: 124–126 °C; Rf = 0.47 (EtOAc: n-Hexane 2:3); ^{1}H NMR (500 MHz, DMSO-d_6) δ 8.54 (s, 1H), 7.73 (d, $J = 7.6$ Hz, 1H), 7.67–7.61 (m, 2H), 7.29–7.23 (m, 2H), 6.78 (d, $J = 2.3$ Hz, 1H), 6.52 (s, 1H), 5.38 (s, 2H), 3.47 (q, $J = 7.0$ Hz, 6H), 2.71 (s, 4H), 2.36 (s, 3H), 1.12 (t, $J = 7.0$ Hz, 6H); ^{13}C NMR (125 MHz, DMSO-d_6) δ 174.12, 157.80, 156.68, 153.43, 150.84, 146.27, 136.51, 133.96, 129.87, 129.21, 119.65, 119.24, 114.16, 106.54, 98.41, 58.59, 43.85, 28.16, 20.41, 11.68. LC-MS $[M + H]^+$; 516.61: Elemental analysis, Calculated,%: $C_{27}H_{28}N_6O_3S$: C, 62.77; H, 5.46; N, 16.27; Found %: C, 62.73; H, 5.42; N, 16.24;

2-(5-(2-((1-(3-acetylphenyl)-1H-1,2,3-triazol-4-yl) methoxy)-4-(diethylamino)phenyl)-1,3,4-thiadiazol-2-yl) cyclopentane-1,3-dione **(9j)**: Yield 63%, mp: 127–129 °C; Rf = 0.35 (EtOAc: n-Hexane 2:3); ^{1}H NMR (500 MHz, DMSO-d_6) δ 8.64 (s, 1H), 8.15 (s, 1H), 7.83 (d, $J = 1.3$ Hz, 1H), 7.73 (d, $J = 7.6$ Hz, 1H), 7.68 (d, $J = 1.4$ Hz, 1H), 7.59 (dd, $J = 7.3$, 7.3 Hz, 1H), 6.78 (d, $J = 2.3$ Hz, 1H), 6.52 (s, 1H), 5.38 (s, 2H), 3.47 (q, $J = 7.0$ Hz, 4H), 2.71 (s, 4H), 2.62 (s, 3H), 1.12 (t, $J = 7.0$ Hz, 6H); ^{13}C NMR (125 MHz, DMSO-d_6) δ 196.85, 174.14, 157.82, 156.70, 153.45, 150.86, 146.37, 137.58, 137.05, 129.23, 129.20, 125.54, 121.49, 119.02, 118.80, 114.18, 106.56, 98.43, 58.61, 43.87, 28.18, 26.06, 11.70. LC-MS $[M + H]^+$; 544.62: Elemental analysis, Calculated,%: $C_{28}H_{28}N_6O_4S$: C, 61.75; H, 5.18; N, 15.43; Found %: C, 61.71; H, 5.14; N, 15.41;

2-(5-(2-((1-(4-acetylphenyl)-1H-1,2,3-triazol-4-yl) methoxy)-4-(diethylamino)phenyl)-1,3,4-thiadiazol-2-yl) cyclopentane-1,3-dione **(9k)**: Yield 68%, mp: 131–133 °C; Rf = 0.34 (EtOAc: n-Hexane 2:3); ^{1}H NMR (500 MHz, DMSO-d_6) δ 8.59 (s, 1H), 7.95–7.89 (m, 2H), 7.77–7.71 (m, 3H), 6.78 (d, $J = 2.3$ Hz, 1H), 6.52 (s, 1H), 5.38 (s, 2H), 3.47 (q, $J = 7.0$ Hz, 4H), 2.71 (s, 4H), 2.56 (s, 3H), 1.12 (t, $J = 7.0$ Hz, 6H); ^{13}C NMR (125 MHz, DMSO-d_6) δ 196.05, 174.08, 157.76, 156.64, 153.39, 150.80, 146.23, 137.51, 134.71, 129.90, 129.17, 119.36, 119.16, 114.12, 106.50, 98.37, 58.55, 43.81, 28.12, 25.70, 11.64. LC-MS $[M + H]^+$;544.62: Elemental analysis, Calculated,%: $C_{28}H_{28}N_6O_4S$: C, 61.75; H, 5.18; N, 15.43; Found %: C, 61.71; H, 5.14; N, 15.41;

2-(5-(4-(diethylamino)-2-((1-(4-nitrophenyl)-1H-1,2,3-triazol-4-yl)methoxy)phenyl)-1,3,4-thiadiazol-2-yl)cyclopentane-1,3-dione **(9l)**: Yield 70%, mp: 137–139 °C; Rf = 0.34 (EtOAc:n-Hexane 2:3); ^{1}H NMR (500 MHz, DMSO-d_6) δ 8.57 (s, 1H), 8.37–8.30 (m, 2H), 7.97–7.90 (m, 2H), 7.73 (d, $J = 7.6$ Hz, 1H), 6.78 (d, $J = 2.3$ Hz, 1H), 6.52 (s, 1H), 5.38 (s, 2H), 3.47 (q, $J = 7.0$ Hz, 4H), 2.71 (s, 4H), 1.12 (t, $J = 7.0$ Hz, 6H); ^{13}C NMR (125 MHz, DMSO-d_6) δ 174.10, 157.78, 156.66, 153.41, 150.82, 148.94, 146.32, 138.89, 129.19, 125.32, 120.52, 119.66, 114.14, 106.52, 98.39, 58.57, 43.83, 28.14, 11.66 LC-MS $[M + H]^+$; 547.59: Elemental analysis, Calculated,%: $C_{26}H_{25}N_7O_5S$: C, 57.03; H, 4.60; N, 17.91; Found %: C, 56.98; H, 4.56; N, 17.87;

Supplementary information The online version contains supplementary material available at https://doi.org/10.1007/s00044-023-03132-9.

Acknowledgements All the authors thank the Head, Department of Chemistry, Osmania University, Hyderabad, for providing laboratory facilities. We thank Central Facilities and Research Development (CFRD) analytical team for providing spectral analytical facilities.

Compliance with ethical standards

Conflict of interest The authors declare no competing interests.

References

1. Popova EA, Protas AV, Trifonov RE. Tetrazole derivatives as promising anticancer agents. Anticancer Agents Med Chem. 2018;17. https://doi.org/10.2174/1871520617666170327143148.
2. Siegel RL, Miller KD, Fuchs HE, Jemal A. Cancer statistics, 2022. CA Cancer J Clin. 2022;72:7–33. https://doi.org/10.3322/caac.21708.
3. Cancer. https://www.who.int/news-room/fact-sheets/detail/cancer.
4. Sahoo SK, Ahmad MN, Kaul G, Nanduri S, Dasgupta A, Chopra S. et al. Synthesis and evaluation of triazole congeners of nitrobenzothiazinones potentially active against drug-resistant mycobacterium tuberculosis demonstrating bactericidal efficacy. RSC Med Chem. 2022;13:585–93. https://doi.org/10.1039/D1MD00387A.
5. Gour J, Gatadi S, Pooladanda V, Ghouse SM, Malasala S, Madhavi YV. et al. Facile synthesis of 1,2,3-triazole-fused indolo- and pyrrolo[1,4]diazepines, DNA-binding and evaluation of their anticancer activity. Bioorg Chem. 2019;93:103306. https://doi.org/10.1016/j.bioorg.2019.103306.
6. Stacy DM, Le Quement ST, Hansen CL, Clausen JW, Tolker-Nielsen T, Brummond JW, et al. Synthesis and biological evaluation of triazole-containing N-Acyl homoserine lactones as quorum sensing modulators. Org Biomol Chem. 2013;11:938–54. https://doi.org/10.1039/C2OB27155A.
7. Zuo Z, Liu X, Qian X, Zeng T, Sang N, Liu H. et al. Bifunctional naphtho[2,3- d][1,2,3]triazole-4,9-dione compounds exhibit antitumor effects in vitro and in vivo by inhibiting dihydroorotate dehydrogenase and inducing reactive oxygen species production. J Med Chem. 2020;63:7633–52. https://doi.org/10.1021/acs.jmedchem.0c00512.
8. Mohammed JH, Mohammed AI, Abass SJ. Antibacterial activity importance of 1, 2, 3-triazole and 1, 2, 4-triazole by click chemistry. J Chem Chem Sci. 2015;5:317–324.
9. Mareddy J, Nallapati SB, Anireddy J, Devi YP, Mangamoori LN, Kapavarapu R. et al. Synthesis and biological evaluation of nimesulide based new class of triazole derivatives as potential PDE4B inhibitors against cancer cells. Bioorg Med Chem Lett. 2013;23:6721–7. https://doi.org/10.1016/j.bmcl.2013.10.035.
10. Kumbhare RM, Dadmal TL, Ramaiah MJ, Kishore KSV, Pushpa Valli SNCVL, Tiwari SK. et al. Synthesis and anti-cancer evaluation of novel triazole linked N-(Pyrimidin-2-Yl)Benzo[d] Thiazol-2-amine derivatives as inhibitors of cell survival proteins and inducers of apoptosis in MCF-7 breast cancer cells. Bioorg Med Chem Lett. 2015;25:654–8. https://doi.org/10.1016/j.bmcl.2014.11.083.
11. Shaikh MH, Subhedar DD, Nawale L, Sarkar D, Khan FAK, Sangshetti JN. et al. 1,2,3-triazole derivatives as antitubercular agents: synthesis, biological evaluation, and molecular docking study. Med Chem Commun. 2015;6:1104–16. https://doi.org/10.1039/C5MD00057B.
12. Pasko MT, Piscitelli SC, Van Slooten AD. Fluconazole: a new triazole antifungal agent. DICP. 1990;24:860–7. https://doi.org/10.1177/106002809002400914.
13. Lass-Flörl C. Triazole antifungal agents in invasive fungal infections. Drugs. 2011;71:2405–19. https://doi.org/10.2165/11596540-000000000-00000.
14. Bangalore PK, Vagolu SK, Bollikanda RK, Veeragoni DK, Choudante PC, Misra S. et al. Usnic acid enaminone-coupled 1,2,3-triazoles as antibacterial and antitubercular agents. J Nat Prod. 2020;83:26–35. https://doi.org/10.1021/acs.jnatprod.9b00475.
15. Aouad MR, Mayaba MM, Naqvi A, Bardaweel SK, Al-blew FF, Messali M. et al. Design, synthesis, in silico and in vitro antimicrobial screenings of novel 1,2,4-triazoles carrying 1,2,3-triazole scaffold with lipophilic side chain tether. Chem Cent J. 2017;11:117. https://doi.org/10.1186/s13065-017-0347-4.
16. Głowacka IE, Balzarini J, Wróblewski AE. Design, synthesis, antiviral, and cytotoxic evaluation of novel phosphorylated 1,2,3-triazoles as acyclic nucleotide analogues. Nucleosides Nucleotides Nucleic Acids. 2012;31:293–318. https://doi.org/10.1080/15257770.2012.662611.
17. Alvarez R, Velázquez S, San-Félix A, Aquaro S, De Clercq E, Perno CF. et al. 1,2,3-Triazole-[2',5'-Bis-O-(Tert-Butyldimethylsilyl)-Beta-D- Ribofuranosyl]-3'-Spiro-5"-(4"-Amino-1",2"-Oxathiole 2",2"-Dioxide) (TSAO) analogues: synthesis and anti-HIV-1 activity. J Med Chem. 1994;37:4185–94. https://doi.org/10.1021/jm00050a015.
18. Poulsen S-A, Wilkinson BL, Innocenti A, Vullo D, Supuran CT. Inhibition of human mitochondrial carbonic anhydrases VA and VB with Para-(4-Phenyltriazole-1-Yl)-benzenesulfonamide derivatives. Bioorg Med Chem Lett. 2008;18:4624–7. https://doi.org/10.1016/j.bmcl.2008.07.010.
19. Rajan S, Puri S, Kumar D, Babu MH, Shankar K, Varshney S. et al. Novel indole, and triazole based hybrid molecules exhibit potent anti-adipogenic and antidyslipidemic activity by activating Wnt3a/β-Catenin pathway. Eur J Med Chem. 2018;143:1345–60. https://doi.org/10.1016/j.ejmech.2017.10.034.
20. Praveenkumar E, Gurrapu N, Kumar Kolluri P, Yerragunta V, Reddy Kunduru B, Subhashini NJP. Synthesis, anti-diabetic evaluation and molecular docking studies of 4-(1- aryl-1H-1, 2, 3-triazol-4-yl)-1,4-dihydropyridine derivatives as novel 11-β hydroxysteroid dehydrogenase-1 (11β- HSD1) inhibitors. Bioorg Chem. 2019;90:103056. https://doi.org/10.1016/j.bioorg.2019.103056.
21. Supuran CT, Scozzafava A. Carbonic anhydrase inhibitors. Curr Med Chem Immunol Endocr Metab Agents. 2001;1:61–97. https://doi.org/10.2174/1568013013359131.
22. Subhashini NJP, Praveen Kumar E, Gurrapu N, Yerragunt V. Design and synthesis of imidazole-1, 2,3-triazoles hybrid compounds by the microwave-assisted method: evaluation as an antioxidant and antimicrobial agents and molecular docking studies. J Mol Struct. 2019;1180:618–28. https://doi.org/10.1016/j.molstruc.2018.11.029.
23. Matysiak J, Malinski Z. [2-(2,4-Dihydroxyphenyl)-1,3,4-thiadiazole analogues: antifungal activity in vitro against Candida species]. Bioorg Khim. 2007;33:640–7. https://doi.org/10.1134/s1068162007060106.
24. Matysiak J, Opolski A. Synthesis and antiproliferative activity of N-substituted 2-Amino-5-(2,4-Dihydroxyphenyl)-1,3,4-thiadiazoles. Bioorg Med Chem. 2006;14:4483–9. https://doi.org/10.1016/j.bmc.2006.02.027.
25. Rzeski W, Matysiak J, Kandefer-Szerszeń M. Anti-cancer, neuroprotective activities and computational studies of 2-amino-1,3,4-thiadiazole based compound. Bioorg Med Chem. 2007;15:3201–7. https://doi.org/10.1016/j.bmc.2007.02.041.
26. Tahghighi A, Razmi S, Mahdavi M, Foroumadi P, Ardestani SK, Emami S. et al. Synthesis and anti-leishmanial activity of 5-(5-Nitrofuran-2-Yl)-1,3,4-thiadiazol-2-amines containing N-[(1-Benzyl-1H-1,2,3-Triazol-4-Yl)Methyl] moieties. Eur J Med Chem. 2012;50:124–8. https://doi.org/10.1016/j.ejmech.2012.01.046.
27. Rajak H, Singour P, Kharya MD, Mishra P. A novel series of 2,5-disubstituted 1,3,4-oxadiazoles: synthesis and SAR study for their anticonvulsant activity. Chem Biol Drug Des. 2011;77:152–8. https://doi.org/10.1111/j.1747-0285.2010.01066
28. Hatvate NT, Ghodse SM, Telvekar VN. Metal-free synthesis of 2-aminothiadiazoles via TBHP-Mediated oxidative C-S bond formation. Synth Commun. 2018. https://doi.org/10.1080/00397911.2017.1398330.

29. Pawar, Pratap Y, Kulkarni, Reshma B, Kalure, Swati U. Synthesis and pharmacological screening of some N-substituted pyrrolidine-2,5-dione derivatives as potential antidepressant agentsInternational. J Pharm Front Res. 2012;2:1–13.
30. Nalawade J, Shinde A, Chavan A, Patil S, Suryavanshi M, Modak M, et al. Synthesis of new thiazolyl-pyrazolyl-1,2,3-triazole derivatives as potential antimicrobial agents. Eur J Med Chem. 2019;179:649–59.
31. Cascioferro S, Li Petri G, Parrino B, El Hassouni B, Carbone D, Arizza V. et al. 3-(6-Phenylimidazo [2,1-*b*][1,3,4]thiadiazol-2-yl)-1*H*-indole derivatives as new anticancer agents in the treatment of pancreatic ductal adenocarcinoma. Molecules. 2020;25:329. https://doi.org/10.3390/molecules25020329.
32. Lu Z-H, Gu X-J, Shi K-Z, Li X, Chen D-D, Chen L. Accessing anti-human lung tumor cell line (A549) potential of newer 3,5-disubstituted pyrazoline analogs. Arab J Chem. 2017;10:624–30. https://doi.org/10.1016/j.arabjc.2014.11.002.
33. S AK, Madderla S, Dharavath R, Nalaparaju N, Katta R, Gundu S. et al. Microwave assisted synthesis of N-substituted acridine-1,8-dione derivatives: evaluation of antimicrobial activity. J Heterocycl Chem. 2022;59:1180–90. https://doi.org/10.1002/jhet.4458.
34. Abdulfatai U, Uzairu A, Uba S. Molecular docking and quantitative structure-activity relationship study of anticonvulsant activity of aminobenzothiazole derivatives. Beni-Suef Univ J Basic Appl Sci. 2018;7:204–14. https://doi.org/10.1016/j.bjbas.2017.11.002.
35. Trott O, Olson AJ. AutoDock Vina: improving the speed and accuracy of docking with a new scoring function, efficient optimization, and multithreading. J Comput Chem. 2009. https://doi.org/10.1002/jcc.21334.
36. Nowakowski J, Cronin CN, McRee DE, Knuth MW, Nelson CG, Pavletich NP. et al. Structures of the cancer-related aurora-A, FAK, and EphA2 protein kinases from nano volume crystallography. Structure. 2002;10:1659–67. https://doi.org/10.1016/S0969-2126(02)00907-3.
37. Lim DY, Shin SH, Lee M-H, Malakhova M, Kurinov I, Wu Q. et al. A natural small molecule, catechol, induces c-Myc degradation by directly targeting ERK2 in lung cancer. Oncotarget. 2016;7:35001–14. https://doi.org/10.18632/oncotarget.9223.